

# Androgen Receptor Ligand-Binding Domain Interaction and Nuclear Receptor Specificity of FXXLF and LXXLL Motifs as Determined by L/F Swapping

Hendrikus J. Dubbink, Remko Hersmus, Ashley C. W. Pike, Michel Molier, Albert O. Brinkmann, Guido Jenster, and Jan Trapman

*Departments of Pathology (H.J.D., R.H., M.M., J.T.) and Urology (G.J.), Josephine Nefkens Institute, and Department of Reproduction and Development (A.O.B.), Erasmus MC, 3000 DR Rotterdam, The Netherlands; and Structural Biology Laboratory (A.C.W.P.), Department of Chemistry, University of York, York YO10 5DD, United Kingdom*

The androgen receptor (AR) ligand-binding domain (LBD) binds FXXLF motifs, present in the AR N-terminal domain and AR-specific cofactors, and some LXXLL motifs of nuclear receptor coactivators. We demonstrated that in the context of the AR FXXLF motif many different amino acid residues at positions +2 and +3 are compatible with strong AR LBD interaction, although a preference for E at +2 and K or R at +3 was found. Pairwise systematic analysis of F/L swaps at +1 and +5 in FXXLF and LXXLL motifs showed: 1) F to L substitutions in natural FXXLF motifs abolished AR LBD interaction; 2) binding of interacting LXXLL motifs was unchanged or increased upon L to F substitutions; 3) certain noninteracting LXXLL motifs became strongly AR-interacting FXXLF motifs; whereas 4) other nonbinders remained unaffected by L to F substitutions. All FXXLF motifs, but not the corre-

sponding LXXLL motifs, displayed a strong preference for AR LBD. Progesterone receptor LBD interacted with some FXXLF motifs, albeit always less efficiently than corresponding LXXLL motifs. AR LBD interaction of most FXXLF and LXXLL peptides depended on classical charge clamp residue K720, whereas E897 was less important. Other charged residues lining the AR coactivator-binding groove, K717 and R726, modulated optimal peptide binding. Interestingly, these four charged residues affected binding of individual peptides independent of an F or L at +1 and +5 in swap experiments. In conclusion, F residues determine strong and selective peptide interactions with AR. Sequences flanking the core motif determine the specific mode of FXXLF and LXXLL interactions. (*Molecular Endocrinology* 20: 1742–1755, 2006)

THE ANDROGEN RECEPTOR (AR) is a ligand-activated transcription factor of the nuclear receptor (NR) superfamily. The AR mediates signal transduction by testosterone and 5 $\alpha$ -dihydrotestosterone (DHT). Androgen signaling is crucial for the growth, differentiation, and maintenance of male reproductive tissues as well as for the growth of the majority of prostate cancers (1–4). All NRs possess an essentially identical domain structure, composed of an N-terminal domain (NTD), a central DNA-binding domain (DBD), and a

C-terminal ligand-binding domain (LBD). Transcriptional activation by NRs relies on a largely unstructured activation domain in the NTD (activation function-1, AF-1) and a highly structured, ligand-dependent activation domain in the LBD (AF-2). AF-1 and AF-2 interact with factors that function as molecular scaffolds for the recruitment and assembly of multiprotein transcription complexes at the promoters of target genes (5–8).

Structural studies have shown that NR transactivation involves a major conformational change in the LBD, enabling interaction with various coactivators (for reviews see Refs. 9–11). Upon ligand binding, the highly flexible helix 12 in the LBD becomes stabilized over the ligand-binding pocket. Repositioning of helix 12 yields a hydrophobic coactivator-binding groove lined by LBD helices 3, 4, 5, and 12. This groove represents the interacting surface for short amphipathic  $\alpha$ -helical sequences designated LXXLL motifs (L, leucine; X, any amino acid residue) or NR boxes present in coactivators (12, 13). Docking of LXXLL motifs in the coactivator groove is achieved by hydrophobic interactions of the L residues with amino acid

## First Published Online April 20, 2006

Abbreviations: AF, Activation function; AR, androgen receptor; DBD, DNA-binding domain; DHT, 5 $\alpha$ -dihydrotestosterone; ER $\alpha$ , estrogen receptor  $\alpha$ ; LBD, ligand-binding domain; N/C interaction, interaction between NTD and LBD; NR, nuclear receptor; NTD, N-terminal domain; PR, progesterone receptor; RXR $\alpha$ , retinoid X receptor  $\alpha$ ; SRC1, steroid receptor coactivator 1; TIF2, transcriptional intermediary factor 2; TR $\beta$ 1, thyroid hormone receptor  $\beta$ 1; UAS, upstream activating sequence; VDR, vitamin D receptor.

***Molecular Endocrinology* is published monthly by The Endocrine Society (<http://www.endo-society.org>), the foremost professional society serving the endocrine community.**

residues in the groove and hydrogen bonding of the LXXLL peptide backbone with charged glutamic acid and lysine residues at opposite ends of the groove (for reviews see Refs. 10 and 14). LXXLL motifs within cofactors display different affinities for distinct NRs (15–21). The variable amino acid residues in or directly flanking the core LXXLL sequence determine NR LBD preference.

A small number of AR LBD interacting LXXLL motifs have been described, including transcriptional intermediary factor 2 (TIF2) NR boxes I and III, and the peptides D11 and D30 that originally were identified in phage display screens for estrogen receptor- $\alpha$  (ER $\alpha$ )-binding motifs (22–25). We and others have shown that the AR LBD also binds to FXXLF motifs (F, phenylalanine) present in the AR NTD and AR cofactors ARA54, ARA70, and hRAD9 (7, 26–28). Additionally, we have shown that oppositely charged amino acid residues at either end of the coactivator-binding groove, K717, K720, and R726 at one side and E897 at the other, differentially affect binding of the AR FXXLF motif and TIF2 LXXLL motifs (24). Recently, the three-dimensional structures of ligand-bound AR LBDs in complex with several FXXLF and LXXLL peptide motifs have been determined. These structures indicate that the AR LBD can accommodate distinct peptide motifs by induced changes in the shape of the coactivator groove (25, 29, 30).

Current endocrine therapies of metastatic prostate cancer are not curative because they are unable to sufficiently block AR function (2, 31, 32). An alternative or complementary approach to block AR function may be targeting the AR coactivator groove. This study aims at increasing our insight in the binding mode of peptides to the AR groove and their NR specificity. Interaction of the AR LBD with a variety of motifs allows the elucidation of the contribution of core F and L hydrophobic residues to coactivator groove interaction. We performed systematic F/L swaps in three FXXLF and nine LXXLL motifs to study AR LBD interaction of pairs of FXXLF and LXXLL peptides in an identical context of flanking amino acid residues. We also examined the dependence of FXXLF and LXXLL peptides on charged residues lining the AR coactivator groove and the NR LBD selectivity of the FXXLF peptides. Our results demonstrate that, in essentially all peptides, the AR LBD favors F residues at the core +1 and +5 positions above L residues for strong interaction. Positions +2 and +3 allowed a wide variety of amino acid residues. Bulky F residues at +1 and +5 were important determinants of AR specificity. AR LBD binding of virtually all FXXLF and LXXLL peptides depended on the classic charge clamp residue K720, whereas E897 was only essential in a subset of the peptides. K717 and R726 modulated optimal peptide interaction in an indirect manner. Finally, we observed that the overall dependence on these charged amino acid residues of corresponding FXXLF and LXXLL peptides was largely identical.

## RESULTS

### Differential Effects of F to L and L to F Swaps in F/LXXLF/L on Interaction with AR LBD

Crystal structures of AR LBD in complex with short peptides derived from the FXXLF-containing regions of AR and ARA70 and the NR box III LXXLL region of TIF2 showed a different mode of FXXLF- and LXXLL-mediated interaction (29, 30). Previously, we obtained contrasting data on the effect of F to L and L to F substitutions at positions +1 and +5 in a given amino acid context (24). Converting the AR FXXLF motif into an LXXLL motif interfered with AR LBD interaction whereas introduction of F residues at positions +1 and +5 in the context of TIF2 LXXLL NR boxes I and III was allowed and could even enhance interaction (24). To further increase our understanding of the AR LBD interaction capacities of F to L- and L to F-substituted FXXLF and LXXLL motifs, respectively, we applied yeast- and mammalian cell-based protein interaction assays. Yeast two-hybrid assays allowed 1) direct comparison of peptide binding to different NR LBDs linked to the same GAL4-transactivation domain and 2) bulk screening for AR LBD-interacting peptides (see below). The mammalian one-hybrid system enabled interaction studies with full-length AR, thereby avoiding possible artifacts introduced by splitting AR into two separate domains.

First, the influence of F to L substitutions in FXXLF motifs of the AR cofactors ARA54 and ARA70 and L to F swaps in p160 coactivator SRC1 (steroid receptor coactivator 1) LXXLL motifs, NR boxes I, II, III and IV, and the LXXLL peptides D11 and D30 (Figs. 1 and 2A) were assayed in a yeast two-hybrid readout system using the GAL4DBD-AR LBD fusion protein as bait. All peptides were expressed to similar levels (Fig. 2B). ARA54 and ARA70 FXXLF motifs interacted well with the AR LBD (Fig. 2C). F to L substitutions in the ARA54 and ARA70 peptides completely abrogated interaction with the AR LBD (Fig. 2C and Table 1). Similar data were found for the AR FXXLF motif (Fig. 2C and Ref. 24), indicating that in these three cases F to L swaps interfered with AR LBD interaction (Table 1). Of the LXXLL motifs tested, only D11 and D30 interacted with AR LBD (Fig. 2D and Table 1). L to F swaps of SRC1 boxes I–IV, D11, and D30 showed three types of interactions. In the first category, both the LXXLL and corresponding FXXLF variants strongly interacted with the AR LBD (D11 and D30, Table 1). L to F substitutions of these peptides can even result in enhanced AR LBD binding (Fig. 2D). Second, two noninteracting LXXLL peptides, SRC1 boxes I and IV, were converted into strong AR LBD-interacting peptides upon L to F replacement. Third, neither the LXXLL nor the corresponding FXXLF variant displayed any AR LBD interaction (SRC1 boxes II and III; Fig. 2D and Table 1).

		-1	+1		+5	+6
<b>AR</b>	17-K T Y R G A	<b>F/L</b>	Q N	<b>L</b>	<b>F/L</b>	Q S V R E-32
<b>ARA54</b>	448-D P G S P C	<b>F/L</b>	N R	<b>L</b>	<b>F/L</b>	Y A V D V-463
<b>ARA70</b>	322-R E T S E K	<b>F/L</b>	K L	<b>L</b>	<b>F/L</b>	Q S Y N V-337
<b>TIF2 Box I</b>	636-S K G Q T K	<b>L/F</b>	L Q	<b>L</b>	<b>L/F</b>	T T K S D-650
<b>TIF2 Box II</b>	684-K E K H K I	<b>L/F</b>	H R	<b>L</b>	<b>L/F</b>	Q D S S S-699
<b>TIF2 Box III</b>	739-K K E N A L	<b>L/F</b>	R Y	<b>L</b>	<b>L/F</b>	D K D D T-754
<b>SRC1 Box I</b>	627-S Q T S H K	<b>L/F</b>	V Q	<b>L</b>	<b>L/F</b>	T T T A E-642
<b>SRC1 Box II</b>	684-T A R H K I	<b>L/F</b>	H R	<b>L</b>	<b>L/F</b>	Q E G S P-699
<b>SRC1 Box III</b>	743-S K D H Q L	<b>L/F</b>	R Y	<b>L</b>	<b>L/F</b>	D K D E K-758
<b>SRC1 Box IV</b>	1427-P Q A Q Q K S L	<b>L/F</b>	Q Q	<b>L</b>	<b>L/F</b>	T E *-1441
<b>D11</b>	E S G S S R	<b>L/F</b>	M Q	<b>L</b>	<b>L/F</b>	M A N D L
<b>D30</b>	P T H S S R	<b>L/F</b>	W E	<b>L</b>	<b>L/F</b>	M E A T P

**Fig. 1.** Amino Acid Sequences of FXXLF and LXXLL Peptides and F/L and L/F Swapped Variants Used in This Study and in Ref. 24. Positions in the corresponding full-length proteins are indicated. D11 and D30 are 16-mers deduced from synthetic ER $\alpha$ -binding LXXLL peptides selected in phage display screens (22). The asterisk indicates a natural stop codon.

Importantly, none of the LXXLL peptides interacted with AR LBD if the corresponding FXXLF variant could not interact.

Next, we examined the effects of F to L and L to F substitutions on interaction with full-length AR containing an inactivated FXXLF motif (F23L/F27L-AR) in transfected Hep3B cells. The FXXLF motif in full-length AR was inactivated to circumvent competition between this motif and individual peptides for AR LBD (24). F to L substitutions abolished interaction of the AR, ARA54, and ARA70 FXXLF peptides with F23L/F27L-AR (Fig. 3A). L to F swaps in SRC1 boxes I and IV LXXLL peptides yielded strongly interacting peptides, and the FXXLF variants of D11 and D30 LXXLL peptides retained their strong interaction capacity (Fig. 3B). Although SRC1 box IV displayed some interaction with F23L/F27L-AR, the results essentially confirmed the yeast protein interaction assay (Fig. 2, C and D).

Taken together, the results showed that F/L swaps in natural FXXLF motifs were not compatible with AR LBD interaction. In contrast, in all cases L/F swaps were permitted in interacting LXXLL peptides and mostly increased their binding properties. In addition, some noninteracting LXXLL peptides gained the capacity to bind AR LBD. Because the binding capacity of distinct FXXLF peptides for AR LBD differed and not all L/F swaps were able to convert noninteracting LXXLL peptides into interacting peptides, the ability and the strength of AR LBD interaction strongly depends on the nature of sequences flanking the core motif. Although some LXXLL peptides bind AR LBD, in most cases L residues at positions +1 and +5 do not give rise to robust interaction with AR LBD.

#### AR LBD-Interacting Peptides Selected from the AR FXXLF Motif Randomly Mutated at +2 and +3

Crystal structures of AR LBD in complex with distinct peptides showed that amino acid residues at positions +2 and +3 are solvent exposed (25, 29, 30). To define the specific amino acid requirements at these positions, we carried out a yeast two-hybrid screen using an AR FXXLF peptide expression library randomized at +2 and +3, and linked to Gal4TAD, and Gal4DBD-AR.LBD as bait (see *Materials and Methods*). Interacting peptides were selected based on rapid growth of blue yeast colonies in selective medium. Peptide sequences of approximately 100 of the most rapidly growing blue colonies were determined, and AR LBD interaction was assessed in a liquid  $\beta$ -galactosidase assay. Many different amino acid combinations at +2 and +3 turned out to give strong interactions (data not shown). Table 2 summarizes  $\beta$ -galactosidase activities of 10 strongly interacting peptides that were selected more than once from the library. AR FQNLFF is added as a control. Most of the peptides contained an E at +2; positively charged K or R was preferred at +3. No other pronounced preferences were observed. All peptides were equally expressed (data not shown). Mammalian one-hybrid assays of the selected peptides with wild-type full-length AR confirmed the yeast data (Table 2).

#### Differential Influence of Charged Residues in the AR Coactivator Groove on Peptide Binding

In previous functional studies, we have shown that the canonical AR charge clamp residue K720 is of major

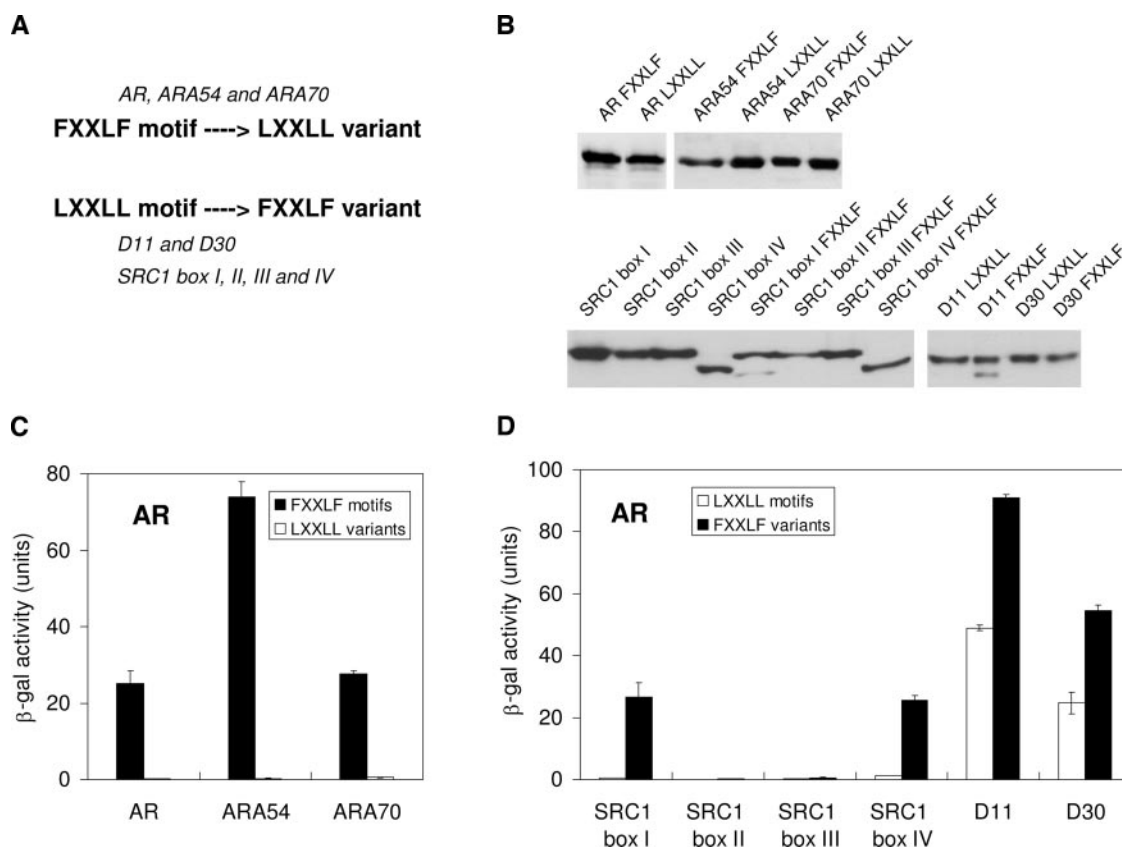


**Fig. 2.** Differential Effects of F to L and L to F Swaps in F/LXXLF/L Interaction  
 A, AR LBD interaction studies were performed with a panel of F to L- and L to F-substituted FXXLF and LXXLL motifs, respectively. Figure 1 shows the corresponding amino acid sequences of the peptides used in this study. B, Western blot analysis of the indicated Gal4AD-peptide fusion proteins expressed in yeast and stained with antibodies against Gal4AD. C, Yeast two-hybrid experiments of Gal4DBD-AR LBD fusion protein with Gal4AD fused to naturally occurring FXXLF motifs and their LXXLL variants. D, Yeast two-hybrid experiments of Gal4DBD-AR LBD fusion protein with Gal4AD fused to naturally occurring and synthetic LXXLL motifs and their FXXLF variants. All yeast two-hybrid experiments were performed in the presence of 1 μM DHT or vehicle. Only results in the presence of hormone are shown. In the absence of hormone, hardly any β-galactosidase activity could be measured. Yeast Y190 transformants expressing solely Gal4DBD-AR LBD fusion proteins did not show any activity in the presence of hormone. Each bar represents the mean β-galactosidase activity of two representative independent experiments (±sd).

importance for AR LBD interaction with TIF2 LXXLL boxes I and III and that E897 is essential for AR FXXLF binding. Two other positively charged residues located at the K720 end of the coactivator-binding groove, K717 and R726, modulate binding of these peptides (24). Structural studies of AR LBD demonstrated that FXXLF motifs fully engage the charge clamp, making hydrogen-bonding interactions with both K720 and E897, whereas LXXLL motifs interact only with K720 (25, 29, 30).

To clarify the apparent discrepancy between the functional studies and the structural information, we extended the examination of the contribution of charged LBD residues in the coactivator groove on FXXLF and LXXLL interaction. We examined the AR-interacting LXXLL peptides D11 and D30, and TIF2 boxes I and III, the FXXLF motifs of ARA54 and ARA70, and the FXXLF variants of TIF2 boxes I and III, SRC1 boxes I and IV, D11 and D30 (see Fig. 1 for se-

quences). Functional interactions were assessed in the mammalian protein interaction assay using F23L/F27L-AR containing single, double, or triple alanine substitutions at positions K717, K720, and R726 or an alanine substitution at position E897. As shown previously, all AR mutants displayed ligand-binding affinities and dissociation rates similar to those of F23L/F27L-AR (24).

First, we studied the effect of alanine substitutions of the classic charged clamp residues E897 and K720 on FXXLF and LXXLL interaction. Figure 4 and Table 3 show that E897A substitution led to at least a 2-fold reduction in the binding capacity of AR-interacting peptides ARA54 FXXLF, ARA70 FXXLF, SRC1 box I FXXLF, and SRC1 box IV FXXLF. It is noteworthy that none of the LXXLL variants of these motifs interacted with AR LBD (Fig. 3). TIF2 box III was the only LXXLL-containing peptide that depended on E897 for AR LBD interaction (Fig. 5 and Table 3). E897A substitution

**Table 1.** Context-Dependent AR LBD Interaction of FXXLF and LXXLL Peptides

Context	Interaction Pattern of Peptide Pair				Ref.
	FXXLF I <sup>a</sup> LXXLL NI	LXXLL NI FXXLF I	LXXLL I FXXLF I	LXXLL NI FXXLF NI	
AR	+ <sup>b</sup>				Ref. 24
ARA 54	+				This study
ARA 70	+				This study
TIF2 I			+		Ref. 24
TIF2 II				+	Ref. 24
TIF2 III			+		Ref. 24
SRC1 I		+			This study
SRC1 II				+	This study
SRC1 III				+	This study
SRC1 IV		+			This study
D11			+		This study
D30			+		This study

Corresponding amino acid sequences are shown in Fig. 1.

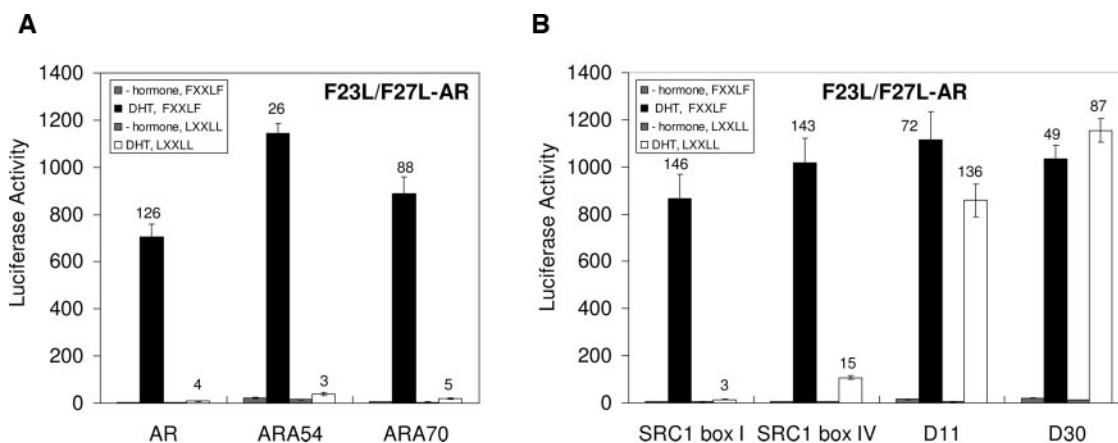
<sup>a</sup> I and NI indicate the interacting and noninteracting variant, respectively. The *upper* motif represents the wild-type motif and the *lower* motif indicates the F/L- or L/F-swapped peptide.

<sup>b</sup> Indicates interaction according to the indicated pattern. Note that no peptide pair has been observed that interacted as LXXLL but not as FXXLF peptide.

hardly affected binding of all other FXXLF and LXXLL peptides (Fig. 5). In contrast, sole K720A substitution was sufficient to severely reduce binding of most FXXLF or LXXLL peptides, except ARA70 FXXLF, D30 LXXLL, and D30 FXXLF (Figs. 4 and 5 and Table 3).

The K717A substitution reduced binding of TIF2 boxes I and III LXXLL peptides and TIF2 box III FXXLF. R726A substitution strongly reduced binding of both L- and F-containing TIF2 box III motifs (Fig. 5, A–D). In all other cases, the single K717A or R726A substitutions had little or no effect on peptide binding (Figs. 4 and 5 and Table 3). Although individual K720A, R726A,

or K717A substitutions did not affect binding of AR LBD to ARA70 FXXLF, D30 LXXLL, and D30 FXXLF, binding strongly decreased upon double K720A/R726A substitutions; K717A/K720A double mutations strongly reduced AR LBD interaction of D30 LXXLL and FXXLF variants. If all three mutations were combined (K717A/K720A/R726A), peptide interaction with AR LBD was completely abolished. Importantly, comparison of the interaction patterns of the LXXLL and FXXLF variants of TIF2 boxes I and III, D11, and D30 with the single, double, and triple AR LBD mutants showed a strikingly similar overall

**Fig. 3.** Effect of L to F and F to L Swaps on AR Interaction in Mammalian Cells

Interaction of AR, ARA54, and ARA70 FXXLF motifs and corresponding LXXLL variants (panel A) and SRC1 boxes I and IV, D11, and D30 LXXLL motifs and corresponding FXXLF variants (panel B) with F23L/F27L-substituted full-length AR as tested in mammalian one-hybrid experiments (see for peptides, Fig. 1). Hep3B cells were cotransfected with expression constructs for F23L/F27L-AR and Gal4DBD-peptide fusion proteins and a (UAS)4 TATA luciferase reporter plasmid. All mammalian one-hybrid experiments were performed in the presence of 0.1  $\mu$ M DHT or vehicle. DHT-dependent transactivation was not observed in the absence of the Gal4DBD-peptide fusion proteins. Each bar represents the mean ( $\pm$ SD) luciferase activity of two representative independent experiments. Mean fold inductions are indicated above bars.

**Table 2.** AR LBD Interaction of the AR FXXLF Motif and Selected Variants with Amino Acid Substitutions at Positions +2 and +3

Amino Acid Sequence	Yeast assay		Mammalian Assay (fold induction)
	No. of Clones <sup>a</sup>	$\beta$ -Gal Activity (units)	
F QN LF		44	38
F ET LF	2	80	50
F ER LF	3	71	76
F EL LF	5	56	47
F EQ LF	3	56	63
F EK LF	9	50	76
F ES LF	3	49	63
F AR LF	2	47	91
F AQ LF	2	44	59
F EC LF	3	30	60
F QH LF	2	21	35

<sup>a</sup> Indicates the frequency that peptide sequences were identified in the yeast two-hybrid screen. Shown are  $\beta$ -galactosidase activities and fold inductions by DHT of representative yeast two-hybrid and mammalian one-hybrid assays, respectively. In yeast assays hardly any  $\beta$ -galactosidase activity was measured in the absence of hormone. Mammalian one-hybrid assays were performed with wild-type full-length AR as described in *Materials and Methods*. Control interactions with the wild-type AR FQNLF motif are indicated.

dependence on E897, K720, K717, and R726 (Fig. 5 and Table 3).

Taken together, interaction of distinct peptides differentially depended on K720 and E897 of AR LBD. E897, to varying degrees, is involved in binding of half of the peptides. K720 is involved in interaction with all peptides, which in some cases is only evident if K717 or R726 are simultaneously mutated. Reduced binding of double mutants for some peptides and complete lack of binding of all peptides by the triple mutant K717/K720/R726 indicate that K717 and R726 modulate peptide binding. Amino acid residues flanking peptide positions +1 and +5 seem to determine which amino acid residues in the AR LBD play the major role in peptide interaction, because the overall dependence of FXXLF and LXXLL variants of identical peptides on charged groove residues is very similar.

### FXXLF Peptides Preferentially Interact with AR LBD

Previously, we have demonstrated that ER $\alpha$  LBD is unable to bind the AR FXXLF motif and L/F-substituted TIF2 boxes I and III due to the shallow nature of its coactivator groove (24). However, limited data are available on interaction of FXXLF motifs with other NRs. To address this issue we studied the interaction of the AR FXXLF motif in the yeast two-hybrid readout system using GAL4DBD-NR LBD fusion proteins as bait. Figure 6A demonstrates that no interaction was found with LBDs of ER $\alpha$ , retinoid X receptor- $\alpha$  (RXR $\alpha$ ), thyroid hormone receptor- $\beta$ 1 (TR $\beta$ 1), and vitamin D

receptor (VDR) and that a weak interaction was only observed with progesterone receptor (PR) LBD. Western blot analysis showed that all Gal4DBD-NR LBD fusion proteins were properly expressed (Fig. 6B). All GAL4DBD-NR LBD fusion proteins adopted an active conformation upon binding of their cognate ligands because interactions were found with at least one of the TIF2 NR boxes I, II, or III fused to Gal4AD in a parallel experiment (data not shown).

We extended the NR LBD studies using the panel of FXXLF and LXXLL peptides shown in Fig. 1. None of the FXXLF peptides interacted with LBDs of ER $\alpha$ , RXR $\alpha$ , TR $\beta$ 1, and VDR, although these LBDs differentially interacted with corresponding LXXLL peptides (data not shown). However, PR LBD could interact with the ARA70 FXXLF motif and the FXXLF variants of TIF2 box I, SRC1 box I and IV, D11, and D30, although always to a lesser extent than the corresponding LXXLL peptides (Fig. 6C). F to L swaps in the ARA70 motif yielded a better interacting peptide, underscoring the LXXLL preference of PR (Fig. 6C). In conclusion, F residues at positions +1 and +5 strongly contributed to preferential and strong interaction with AR LBD and prohibited binding to most other NR LBDs.

## DISCUSSION

The FXXLF motif in the AR NTD is essential for functional AR N/C interaction (interaction between NTD and LBD) (7, 24, 26). Previously, we have shown by homology modeling of the AR LBD/FXXLF complex that the bulky F residues of the AR FXXLF motif perfectly fit in a complementary large hydrophobic AR coactivator-binding groove, whereas the shallower ER $\alpha$  groove explained why ER $\alpha$  does not bind FXXLF peptides (24). Here we systematically assayed F to L and L to F swaps at +1 and +5 positions of FXXLF and LXXLL peptides for AR LBD interactions. We provide evidence that F residues are essential for robust AR LBD binding, that AR prefers FXXLF above LXXLL peptides, and that F residues are essential for the NR specificity of FXXLF peptides. We also demonstrated that a wide variety of amino acid residues could be present at positions +2 and +3. We observed that PR binds certain FXXLF motifs albeit with much lower binding capacity than corresponding LXXLL peptides. Distinct FXXLF and LXXLL peptides were found to be differentially dependent on the charged amino acid residues K717, K720, R726, and E897 in AR LBD. In addition, AR-interacting FXXLF and LXXLL variant peptides displayed a similar overall dependency on these charged residues.

We found a striking preference of FXXLF over LXXLL peptides for AR LBD. All F to L substitutions in interacting natural FXXLF motifs yielded noninteracting peptides, whereas +1 and +5 L to F substitutions of several noninteracting LXXLL motifs resulted in AR-interacting peptides (Table 1 and Fig. 2). Only four of

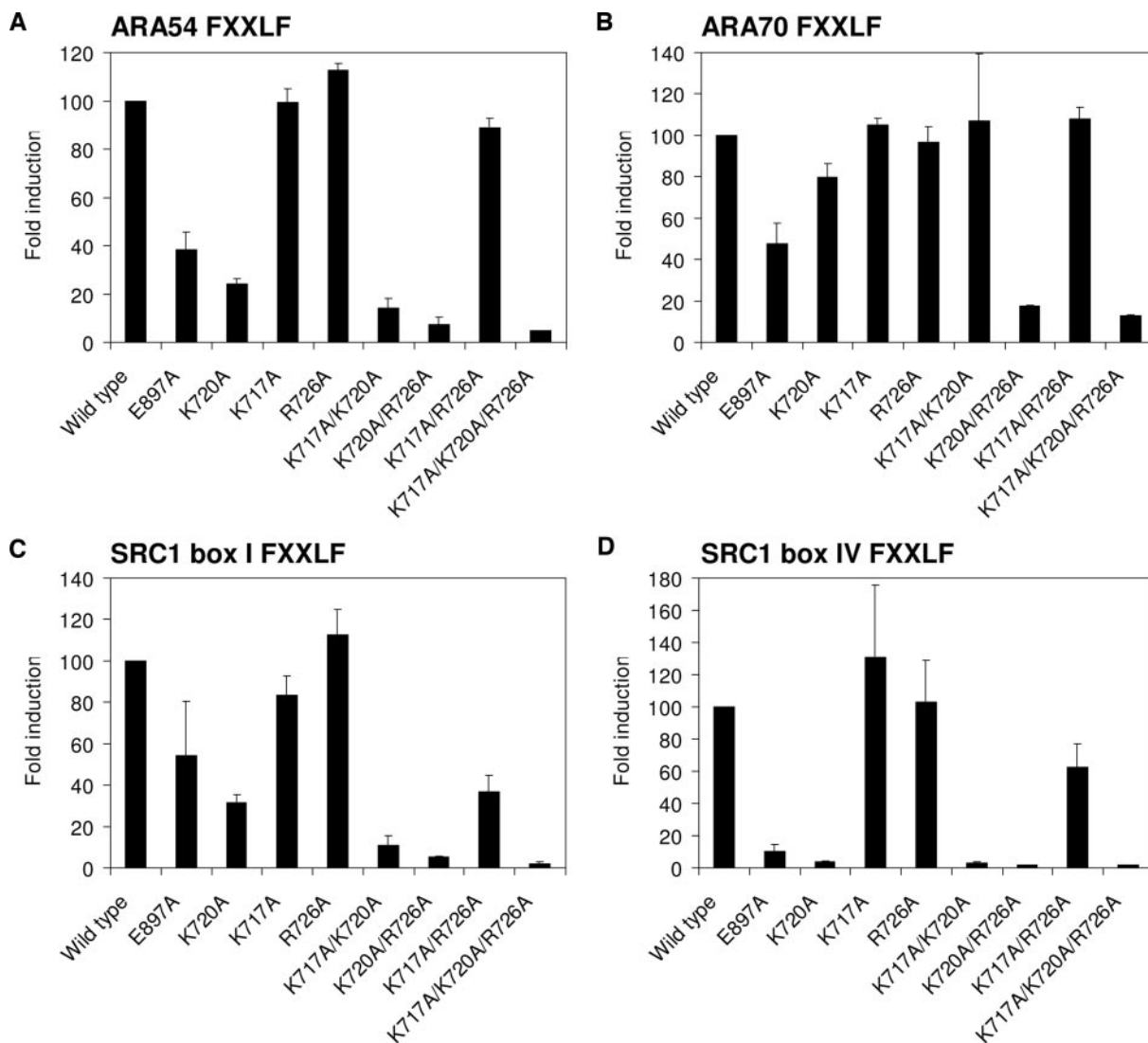


**Fig. 4.** Differential Influence of Charged Residues in the AR Coactivator Groove on Peptide Binding

Interaction of the peptides ARA54 FXXLF (A), ARA70 FXXLF (B), SRC1 box I FXXLF (C), and SRC1 box IV FXXLF (D), with the indicated wild-type and mutant F23L/F27L-AR as tested in mammalian one-hybrid assays (see for peptides, Fig. 1). Experiments were performed according to the legend to Fig. 3. Each bar represents the mean ( $\pm$ SD) luciferase activity of two representative independent experiments. In each independent experiment, fold induction of the interaction between the indicated peptide and F23L/F27L-AR was arbitrarily set to 100.

12 LXXLL peptides tested showed AR binding. Interestingly, none of the peptide contexts allowed AR binding of the LXXLL peptide and not of its corresponding FXXLF variant (Table 1). Also phage display screens for AR LBD interacting peptides yielded hardly any LXXLL peptides in contrast to FXXLF peptides (25, 33), and a recent focused screen of an LXXLL library yielded only two interacting peptides (34). Crystal structures of AR LBD in complex with AR FXXLF, ARA70 FXXLF, and TIF2 box III LXXLL motifs and phage display-selected FXXLF and LXXLL peptides indicate an induced fit mechanism that allows the AR coactivator-binding groove to accommodate the F and L residues at positions +1 and +5 (Fig. 7) (25, 29, 30). In contrast to L residues, the bulkier F residues

make optimal hydrophobic interactions with amino acid residues lining the cofactor-binding groove in AR LBD. Amino acids that flank the core motif appear to be the driving force for interacting LXXLL peptides; however, these alone do not appear sufficient to facilitate binding of the majority of LXXLL peptides.

In contrast to the limited number of amino acid changes that are allowed at +1 and +5 of the AR FXXLF motif (24), we here show that at positions +2 and +3 of the motif different combinations of a wide variety of amino acid residues are compatible with efficient AR LBD interaction. Apart from M at +2 and F and Y at +3, we detected all possible amino acid residues, including presumed helix breakers P and G, at these positions in peptides with high binding ca-

**Table 3.** Interaction of Wild-Type (WT) and Mutant AR LBDs with FXXLF and LXXLL Peptides

Peptide	WT	E897A	K720A	K717A	R726A	K717A K720A	K720A R726A	K717A R726A	K717A K720A R726A
AR	+	–	+/-	+	+	+/-	+/-	+	+/-
ARA54	+	+/-	+/-	+	+	–	–	+	–
ARA70	+	+/-	+	+	+	+	–	+	–
SRC1 box I FXXLF	+	+/-	+/-	+	+	–	–	+/-	–
SRC1 box IV FXXLF	+	–	–	+	+	–	–	+/-	–
TIF2 box I	+	+	–	+/-	+	–	–	+/-	–
TIF2 box I FXXLF	+	+	–	+	+	–	–	+	–
TIF2 box III	+	+/-	–	+/-	+/-	–	–	–	–
TIF2 box III FXXLF	+	+/-	–	+/-	+/-	–	–	–	–
D11	+	+	–	+	+	–	–	+/-	–
D11 FXXLF	+	+	+/-	+	+	–	–	+	–
D30	+	+	+	+	+	+/-	+/-	+	–
D30 FXXLF	+	+	+	+	+	+/-	+/-	+	–

Amino acid sequences of peptides are shown in Fig. 1. Peptide interaction with F23L/F27L-AR (WT) is set to 100%; –, <20%; +/-, >20% and <70%; +, >70%.

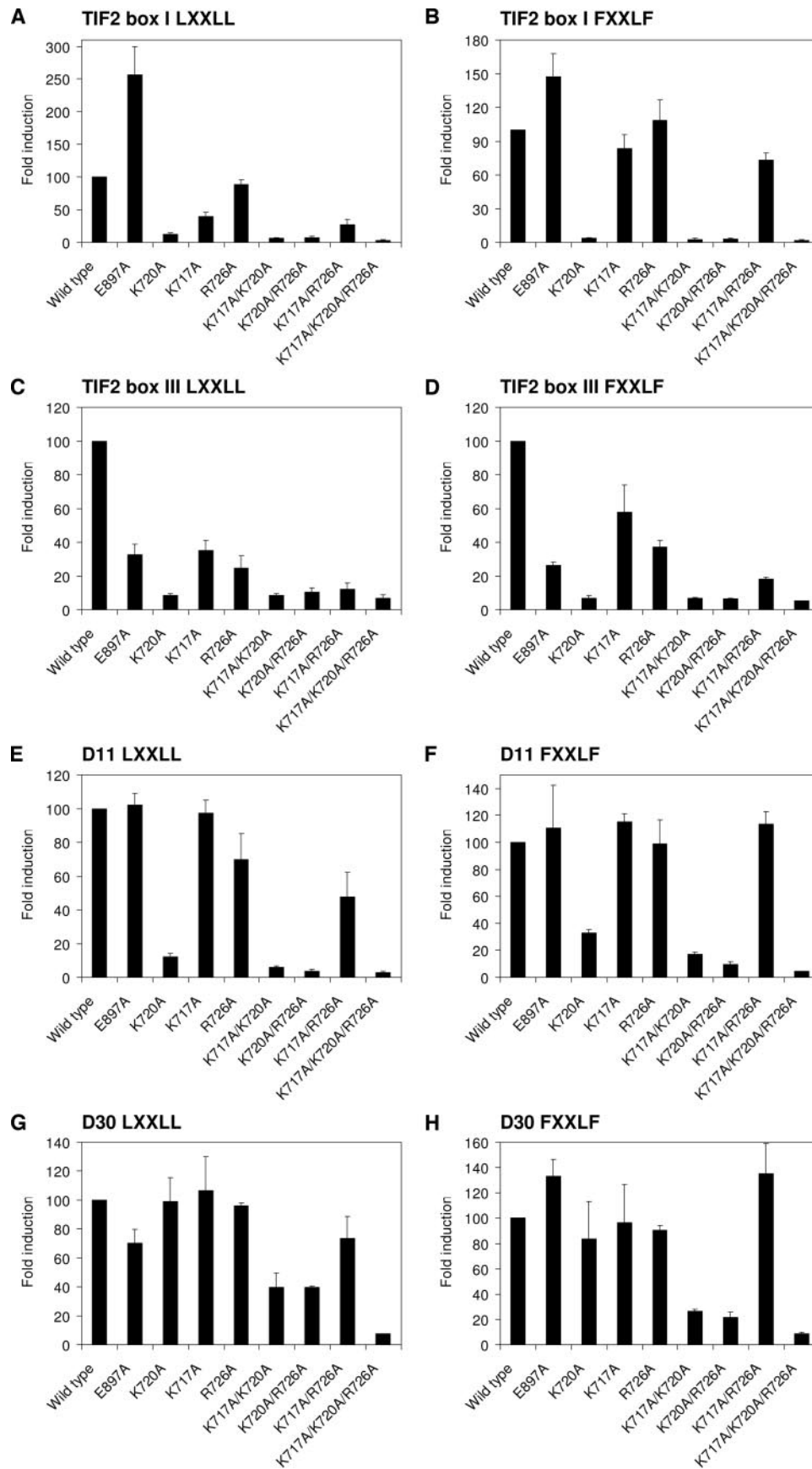
capacity. The observation that many different amino acid residues can occupy the +2 and +3 positions is in agreement with AR LBD-peptide crystal structures, showing that these residues are solvent exposed and do not directly interact with the LBD surface (25, 29). The AR LBD preference for peptides with a negatively charged E at +2 and positively charged K or R at +3 is not fully understood. In this respect it is noteworthy that, like AR, ER $\beta$  prefers binding to phage display-derived LXXLL peptides with positively charged residues at +3; however, TR $\beta$  prefers basic residues at +2 (35). We presume that charged residues at +2 and +3 contribute to a more stable conformation of the peptide.

The crystal structures of AR LBD in complex with FXXLF and LXXLL peptides predict hydrogen bonds between K720 and FXXLF and LXXLL peptides, whereas E897 selectively forms hydrogen bonds with FXXLF peptides. The absence of hydrogen bonds between E897 and LXXLL peptides is due to a shift of these peptides in the groove toward K720, as compared with FXXLF peptides (see Fig. 7). Previously, we have shown that AR FXXLF binding almost completely depends on E897, whereas TIF2 NR LXXLL boxes I and III binding strongly relies on K720 (24). The current functional studies show that there is no strict correlation between binding of FXXLF and LXXLL peptides and E897 or K720 dependency. K720 is of major importance for binding of AR LBD to most FXXLF and LXXLL peptides. In the case of ARA70 FXXLF, D30 LXXLL, and D30 FXXLF, K720 dependency becomes apparent only after an additional mutation of K717 or R726. On the other hand, E897 played a role in interaction of half of the FXXLF peptides, but is of minor importance for LXXLL binding, with TIF2 NR box III LXXLL as an exception (Fig. 5 and Table 3).

The binding requirements for coactivator motifs do not appear to be as straightforward as implied by recent structural studies. Our results suggest that

some of the FXXLF peptides do not form hydrogen bonds with both E897 and K720 and that not all LXXLL peptides interact specifically with K720 as predicted by the available AR LBD/FXXLF and LXXLL crystal structures (Fig. 7) (25, 29, 30). Alternatively, abrogation of interactions by mutation of K720/E897 is differentially compensated by additional, distinct interactions of sequences flanking the core hydrophobic residues with other AR LBD amino acid residues. Evidence to support the existence of such compensating interactions is provided by the observation that K720 mutation does not have a strong effect on binding of the AR FXXLF and ARA70 FXXLF motifs (Fig. 4B), even though in the crystal structures of AR LBD in complex with these motifs K720 is hydrogen bonded to F27 and V30 in the AR FXXLF peptide and to F332 in the ARA70 peptide (Fig. 1) (29, 30). Furthermore, disruption of the hydrogen bonds between AR E897 and the AR FXXLF and ARA70 FXXLF motifs (29, 30) abrogates AR FXXLF interaction (24) but has only a limited effect on ARA70 FXXLF binding (Fig. 4B and Table 3). In addition, the overall dependence on the charged residues in the groove is hardly affected by L to F substitutions of LXXLL peptides, implying that flanking sequences are the main determinants for the observed differential dependency on charged residues (Fig. 5 and Table 3). This similar dependency on charged residues was unexpected given the shifted binding mode adopted by LXXLL peptides in the AR groove, compared with FXXLF-containing motifs (Fig. 7 and Refs. 25 and 29). Based on our results, we propose that, in an identical context, interacting FXXLF and LXXLL motifs have a similar position in the groove, allowing a similar mode of interaction.

Hur *et al.* (25) described various structures of AR LBD in complex with phage display-selected AR-interacting peptides, showing that AR E897 could be differentially involved in interactions with residues flanking the core amino acids at position +1. These



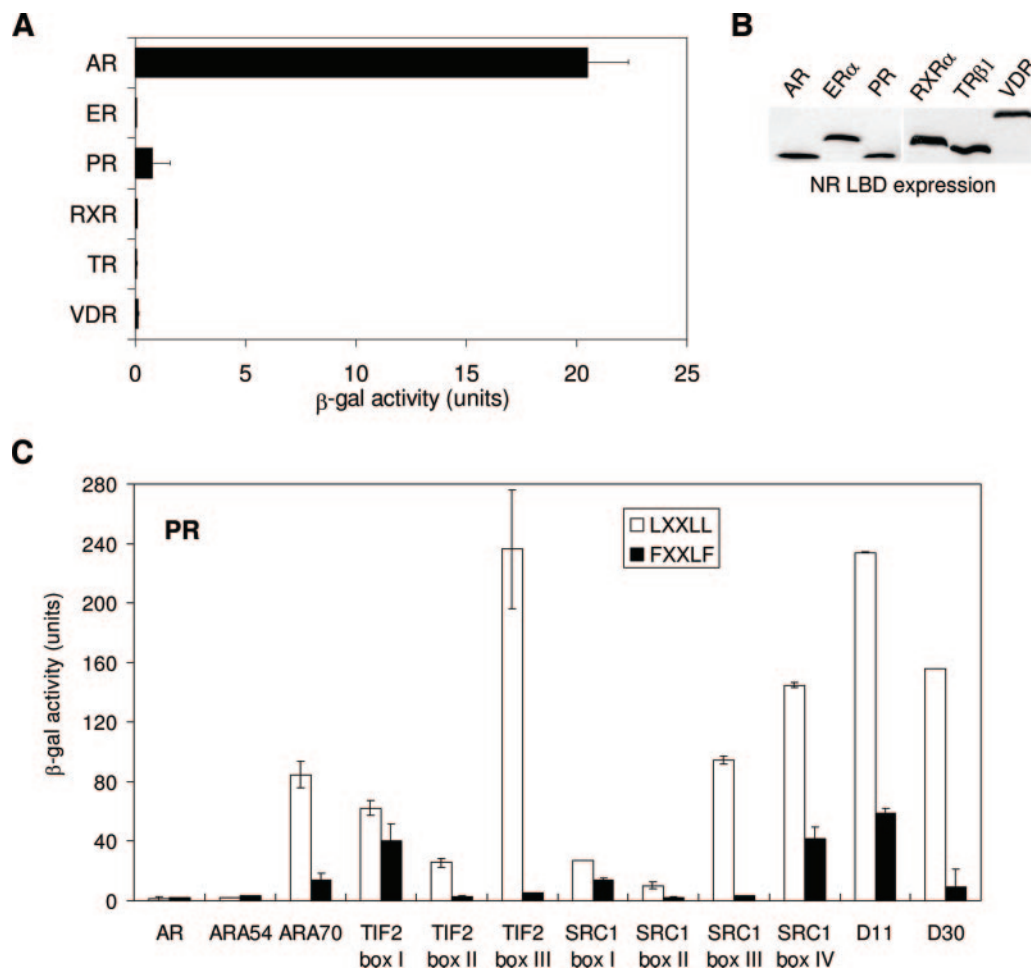


**Fig. 6.** FXXLF Peptides Preferentially Interact with AR LBD

A, Interaction of the AR FXXLF motif with LBDs of AR, ER $\alpha$ , PR, RXR $\alpha$ , TR $\beta$ 1, and VDR. Yeast two-hybrid experiments were performed with Gal4AD-AR FXXLF fusion protein and indicated Gal4DBD-NR LBD fusion proteins. All experiments were performed in the presence of appropriate amounts of hormone (see *Materials and Methods*) or vehicle. Only results in the presence of hormone are shown, because in the absence of hormone hardly any  $\beta$ -galactosidase activity could be measured. Yeast Y190 transformants expressing solely Gal4DBD-NR LBD fusion proteins did not show any activity in the presence of hormone. B, Western blot analysis of the indicated Gal4DBD-NR LBD fusion proteins in yeast, stained with antibodies against Gal4DBD. C, Interaction of paired FXXLF and LXXLL motifs with PR LBD (for peptides see Fig. 1). Yeast two-hybrid experiments were performed according to the legends to Figs. 2 and 6A. Each bar represents the mean  $\beta$ -galactosidase activity of two representative independent yeast two-hybrid experiments ( $\pm$ SD).

include hydrogen bonds of E897 with the side chain and backbone of R-1 of an SRFXXLF peptide and the side chain of S-2 in peptides of a SRFXXFF, SKFXXLW, SRWXXLF, and SRWXXVW signature. The D11 and D30 peptides used in this study have a similar SRL/FXXLL/F signature (Fig. 1). However, E897A substitution did not strongly affect binding of these pep-

tides (Fig. 5, E–H, and Table 3), indicating that E897 interaction with S-2 and R-1 is not essential for peptide binding to the groove.

The exact role of AR K717 and R726 in FXXLF and LXXLL interaction is less clear. These two basic residues flank the charge clamp residue K720 and contribute to the overall positive electrostatic potential at

**Fig. 5.** Similar Dependence on Charged Residues in the AR Coactivator Groove of Paired FXXLF and LXXLL Peptides

Interaction of the peptides TIF2 box I LXXLL (A), TIF2 box I FXXLF (B), TIF2 box III LXXLL (C), TIF2 box III FXXLF (D), D11 LXXLL (E), D11 FXXLF (F), D30 LXXLL (G), and D30 FXXLF (H) with the indicated wild-type and mutant F23L/F27L-substituted AR as tested in mammalian one-hybrid assays (see for peptides, Fig. 1). Experiments were performed according to the legend to Fig. 3. Each bar represents the mean ( $\pm$ SD) luciferase activity of two representative independent experiments. In each independent experiment, fold induction of the interaction between the indicated peptide and F23L/F27L-AR was arbitrarily set to 100.

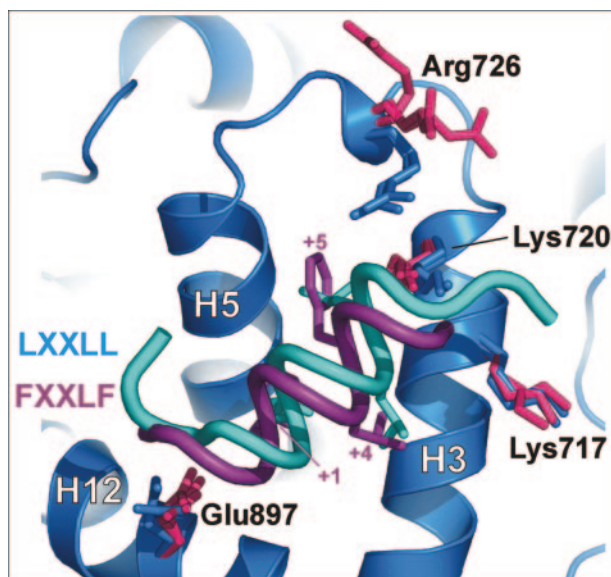


**Fig. 7.** FXXLF and LXXLL Binding Modes to AR LBD as Revealed by x-Ray Crystallography

Close-up view of the coactivator groove of AR is shown to illustrate the distinct modes of binding observed for FXXLF- and LXXLL-containing peptides (25, 29, 30). Helices H3–5 and H12 of AR LBD are drawn schematically in blue. The superposed ARA70 FXXLF and TIF2 NR box III LXXLL peptides are depicted as purple and cyan coils. Orientations of LBD residues analyzed in this study are shown from five independent structures of FXXLF (pink) and LXXLL (blue) peptide complexes. The FXXLF peptide fully engages the charge clamp (K720/E897) whereas the TIF2 NR box III LXXLL peptide is shifted toward the K720 end of the cleft. The coordinates of AR LBD in complex with TIF2 box III LXXLL (Protein Data Bank codes: 1XQ2, 1T63), ARA70 FXXLF (1T5Z), AR FXXLF (1XOW), and phage display FXXLF (1T7R) were superposed using the LBD residues alone for the purposes of this comparison. Figure was generated using PYMOL (<http://pymol.sourceforge.net>).

the upper end of the coactivator groove. R726 is solvent exposed and exhibits multiple side chain conformations directed toward the bound peptide, whereas the side chain of K717 adopts a single conformation in the various crystal structures (Fig. 7). In the majority of these structures, no direct interactions between either K717 or R726 and the bound peptides have been observed. In the case of published LXXLL complexes, R726 is positioned so that it participates in a hydrogen-bonded interaction with the main chain carbonyl of L+5 (Fig. 7) (29, 30). Accordingly, alanine substitutions of either K717 or R726 alone tend to have negligible effects on the efficiency of peptide interaction. However, when combined with K720A, the double mutants exhibited significantly lower binding (Table 3). This suggests that these residues, although dispensable for direct motif recognition, make significant contributions to the overall electrostatic stabilization of motif binding to AR through interaction with the peptide's helix dipole. The basic patch formed by these residues is also required to bind the negatively charged, C-terminal flanking sequences of certain motifs (see Fig. 1). This is perhaps most apparent in the case of L/F variations of TIF2 box III, a motif that has three Asp residues at the carboxy-terminal end, where single mutations at either K717 or R726 appear to have pronounced effects in our functional protein interaction assays (Fig. 5, C and D) (24).

Although the LXXLL peptides used in this study displayed some NR selectivity, none was specific for

one particular NR (data not shown). On the other hand, the FXXLF peptides were highly AR specific. None of the FXXLF peptides showed interaction with other NR LBDs, except for weak PR LBD interaction (Fig. 6 and data not shown). L to F substitutions of AR LBD-interacting LXXLL peptides completely abolished interaction with most other NR LBDs (data not shown and Ref. 24) and decreased interaction capacity with PR LBD (Fig. 6C). It is obvious that F residues are dominant over flanking sequences in AR LBD specificity.

In contrast to AR, PR prefers LXXLL over FXXLF peptides although it does not completely exclude FXXLF binding (Figs. 2 and 6C). The few amino acid differences between AR and PR coactivator-binding grooves, representing AR residues V713, V730, M734, and I898 vs. PR residues L727, I744, I748, and V912, may underlie differential packing of F and L residues in the grooves. In AR LBD these residues, except for V713, contribute to the +1 and +5 pockets and are involved in hydrophobic contacts with the core F and L residues (25, 29). Crystal structures of PR LBD in complex with peptide motifs may shed light on the distinct mode of interaction of PR with FXXLF and LXXLL motifs in comparison with the interaction of similar motifs with the AR LBD.

Different NR LBDs bind distinct repertoires of LXXLL motifs present in interacting proteins (15–21). LXXLL motifs are thus involved in selective binding of coactivators to NR LBDs, although much less specific than

FXXLF motif binding to AR. ARA70 has both a functional FXXLF and LXXLL motif. According to NR preferences of FXXLF and LXXLL motifs, the ARA70 FXXLF motif appeared to be essential for AR interaction and the LXXLL motif mediates interaction with peroxisome proliferator-activated receptor  $\gamma$  (36). Selective recruitment by AR LBD of cofactors with FXXLF motifs, such as ARA54, ARA70, and hRAD9, and less efficient binding with LXXLL-containing cofactors will contribute to functions that discriminate AR from other NRs. FXXLF-mediated N/C interaction may selectively block AR binding to low-affinity cofactors. However, cofactors containing high-affinity FXXLF motifs may successfully compete with AR N/C interaction, as has been demonstrated for hRAD9 (28).

Protein-protein interaction surfaces are suitable targets for small molecules to interfere with activity of key transcription factors and cancer growth (37). Recent studies have shown that specific blocking of P53-MDM2 (38) and Bcl-X<sub>L</sub>/BAK (39) interactions has the potential to induce regression of solid tumors. The AR plays a crucial role in prostate tumor growth. However, current endocrine prostate cancer therapy fails because an initial androgen-dependent tumor progresses into an androgen-independent tumor (2, 31, 32). In most relapsed tumors the AR is still active, indicating that not only the ligand-binding pocket but also other AR surfaces need to be considered as therapeutic targets. The AR coactivator groove represents a well-defined target by interfering with cofactor recruitment and N/C interaction. Our study contributes to an increased understanding of the molecular mode of interaction of AR-binding peptides and can contribute to the development of high-affinity and -specificity AR-blocking drugs inhibiting prostate cancer.

## MATERIALS AND METHODS

### Ligands

DHT, estradiol, deoxycorticosterone, and progesterone were purchased from Steraloids (Wilton, NH); 9-*cis*-retinoic acid was obtained from Sigma Chemical Co. (St. Louis, MO); T<sub>3</sub> and 1,25-dihydroxyvitamin D<sub>3</sub> were kindly provided by George Kuiper and Hans van Leeuwen, respectively.

### Plasmids

Yeast and mammalian expression plasmids encoding Gal4AD-FXXLF or Gal4AD-LXXLL peptide fusion constructs and Gal4DBD-peptide expression constructs, respectively, were generated as described previously (24). The sequences of all peptide expression constructs were verified.

Yeast construct pGalDBD-AR.LBD (AR<sub>661–919</sub>) has been described previously (40). Yeast constructs expressing Gal4DBD fused to LBDs of ER $\alpha$ , PR, RXR $\alpha$ , TR $\beta$ 1, and VDR were generously provided by Michael Stallcup (16). Mutant F23L/F27L-AR constructs used in the mammalian interaction assays have been described previously (24). The upstream activating sequence (UAS)4 TATA luciferase reporter construct was kindly provided by Magda Meesters. The (androgen response element)<sub>2</sub>-E1b-TATA luciferase reporter con-

struct has been described previously as (progesterone response element)<sub>2</sub>-E1b-LUC (41).

### Yeast Protein Interaction Assays and Western Blot Analysis

Y190 yeast cells were transformed with constructs expressing Gal4DBD-NR LBD and Gal4AD-peptide fusion proteins according to the lithium acetate method (42). Liquid culture  $\beta$ -galactosidase assays were performed as described previously (7, 24). Briefly, stationary phase cultures of Y190 yeast transformants grown in appropriate selective medium (0.67% wt/vol yeast nitrogen base without amino acid, 2% glucose, pH 5.8), supplemented with the required amino acids and hormone or vehicle, were diluted in the same culture medium and grown until an OD<sub>600</sub> between 0.7 and 1.2. Next,  $\beta$ -galactosidase activity was determined and calculated as previously described in detail (40).  $\beta$ -Galactosidase activity was expressed in arbitrary units based on culture density, volume of yeast culture tested, absorbance at 420 nm of the enzyme-substrate reaction, and reaction time. Because hardly any activity was measured in the absence of hormone, no background was subtracted from the activity obtained in the presence of hormone. Hormones were applied at 1  $\mu$ M DHT (AR), 0.1  $\mu$ M estradiol (ER $\alpha$ ), 1  $\mu$ M progesterone (PR), 10  $\mu$ M 9-*cis*-retinoic acid (RXR $\alpha$ ), 10  $\mu$ M T<sub>3</sub> (TR $\beta$ 1), and 1  $\mu$ M 1,25-dihydroxyvitamin D<sub>3</sub> (VDR). High hormone concentrations were used to overcome less efficient uptake and/or metabolism by yeast. Expression of Gal4AD and Gal4DBD fusion proteins was assessed by Western blot analysis as described previously (24).

### Mammalian Cell Culture, Transient Transfections, and Luciferase Assay

Hep3B cells were cultured and transfected with constructs expressing full-length AR, Gal4DBD-peptide, and the (UAS)4-TATA luciferase reporter as described previously (24, 43). For transient transfections cells were seeded at a density of  $5 \times 10^4$  cells per well in 24-well plates and grown for 24 h. Four hours before transfection, the medium was replaced by 250  $\mu$ l  $\alpha$ -MEM, supplemented with charcoal-stripped fetal calf serum, antibiotics, and medium with either 0.1  $\mu$ M DHT or vehicle. Transfections were performed in 25  $\mu$ l  $\alpha$ -MEM containing 1  $\mu$ l Fugene 6 (Boehringer Mannheim, Mannheim, Germany), 150 ng (UAS)4 TATA luciferase reporter, 50 ng Gal4DBD-peptide expression construct, and 50 ng AR expression construct per well. After incubation for 24 h, cells were lysed and luciferase activity was assayed as described previously (24, 43). In this system AR recruited to the reporter by the Gal4DBD-peptide fusion protein provides transactivating function. Assays were performed in duplicate in two independent experiments.

### Library Construction and Screening

Random mutagenesis at positions +2 and +3 of the AR FXXLF motif was performed by QuikChange Site-Directed Mutagenesis (Stratagene, La Jolla, CA) using plasmid pACT2-AR 18–30 Q24P/N25P as template. This construct expresses a Gal4AD-AR18–30 peptide, with P substitutions at positions 24 and 25, which cannot interact with the AR LBD. Oligonucleotides used were 5'-ACCTACCGAGGAGCTTTCNNNNNNCTGTTCAGAGCGTGGAA-3' and its complementary strand. The resulting plasmids were transformed to *Escherichia coli* strain XL-1 blue, and 20,000 independent colonies were harvested from which the library DNA was prepared. Appropriate mutagenesis was verified by sequence analyses of randomly selected clones.

The library DNA was transformed to yeast strain Y190 containing pGalDBD-AR.LBD, as described above. A total of

100,000 transformants was plated on selective medium lacking leucine, tryptophan, and histidine and containing X- $\alpha$ -gal (Takara Bio, Otsu, Shiga, Japan), 20 mM 3-amino-1,2,4-triazole, and 1  $\mu$ M DHT. Library plasmids were recovered from colonies, according to the Yeast Protocol Handbook (Takara Bio).

### Acknowledgments

We thank Magda Meesters and Michael Stallcup for generously providing constructs; Drs. Hans van Leeuwen and George Kuiper for providing us with hormones; and Judith van Tol for technical assistance.

Received August 30, 2005. Accepted April 12, 2006.

Address all correspondence and requests for reprints to: Hendrikus J. Dubbink, Department of Pathology, Josephine Nefkens Institute, Erasmus MC, P.O. Box 1738, 3000 DR Rotterdam, The Netherlands. E-mail: h.dubbink@erasmusmc.nl.

Present address for A.C.W.P.: Structural Genomics Consortium, University of Oxford, Botnar Research Centre, Oxford OX3 7LD, United Kingdom.

This work was supported by the Dutch Cancer Society and the European Community's Sixth Framework Program. A.C.W.P. is supported by a Wellcome Trust Career Development Fellowship.

H.J.D., R.H., A.C.W.P., M.M., A.O.B., G.J., and J.T. have nothing to declare.

### REFERENCES

- Quigley CA, De Bellis A, Marschke KB, el-Awady MK, Wilson EM, French FS 1995 Androgen receptor defects: historical, clinical, and molecular perspectives. *Endocr Rev* 16:271–321
- Brinkmann AO, Blok LJ, de Ruyter PE, Doesburg P, Steketeer K, Berrevoets CA, Trapman J 1999 Mechanisms of androgen receptor activation and function. *J Steroid Biochem Mol Biol* 69:307–313
- Heinlein CA, Chang C 2002 Androgen receptor (AR) coregulators: an overview. *Endocr Rev* 23:175–200
- Gelmann EP 2002 Molecular biology of the androgen receptor. *J Clin Oncol* 20:3001–3015
- McKenna NJ, O'Malley BW 2002 Combinatorial control of gene expression by nuclear receptors and coregulators. *Cell* 108:465–474
- Warnmark A, Treuter E, Wright AP, Gustafsson JA 2003 Activation functions 1 and 2 of nuclear receptors: molecular strategies for transcriptional activation. *Mol Endocrinol* 17:1901–1909
- Steketeer K, Berrevoets CA, Dubbink HJ, Doesburg P, Hersmus R, Brinkmann AO, Trapman J 2002 Amino acids 3–13 and amino acids in and flanking the 23FxxLF27 motif modulate the interaction between the N-terminal and ligand-binding domain of the androgen receptor. *Eur J Biochem* 269:5780–5791
- McEwan IJ 2004 Molecular mechanisms of androgen receptor-mediated gene regulation: structure-function analysis of the AF-1 domain. *Endocr Relat Cancer* 11: 281–293
- Moras D, Gronemeyer H 1998 The nuclear receptor ligand-binding domain: structure and function. *Curr Opin Cell Biol* 10:384–391
- Li Y, Lambert MH, Xu HE 2003 Activation of nuclear receptors: a perspective from structural genomics. *Structure* 11:741–746
- Greschik H, Moras D 2003 Structure-activity relationship of nuclear receptor-ligand interactions. *Curr Top Med Chem* 3:1573–1599
- Heery DM, Kalkhoven E, Hoare S, Parker MG 1997 A signature motif in transcriptional co-activators mediates binding to nuclear receptors. *Nature* 387:733–736
- Torchia J, Rose DW, Inostroza J, Kamei Y, Westin S, Glass CK, Rosenfeld MG 1997 The transcriptional co-activator p/CIP binds CBP and mediates nuclear-receptor function. *Nature* 387:677–684
- Nagy L, Schwabe JW 2004 Mechanism of the nuclear receptor molecular switch. *Trends Biochem Sci* 29: 317–324
- Darimont BD, Wagner RL, Apriletti JW, Stallcup MR, Kushner PJ, Baxter JD, Fletterick RJ, Yamamoto KR 1998 Structure and specificity of nuclear receptor-coactivator interactions. *Genes Dev* 12:3343–3356
- Ding XF, Anderson CM, Ma H, Hong H, Uht RM, Kushner PJ, Stallcup MR 1998 Nuclear receptor-binding sites of coactivators glucocorticoid receptor interacting protein 1 (GRIP1) and steroid receptor coactivator 1 (SRC-1): multiple motifs with different binding specificities. *Mol Endocrinol* 12:302–313
- Leers J, Treuter E, Gustafsson JA 1998 Mechanistic principles in NR box-dependent interaction between nuclear hormone receptors and the coactivator TIF2. *Mol Cell Biol* 18:6001–6013
- McInerney EM, Rose DW, Flynn SE, Westin S, Mullen TM, Kronen A, Inostroza J, Torchia J, Nolte RT, Assamunt N, Milburn MV, Glass CK, Rosenfeld MG 1998 Determinants of coactivator LXXLL motif specificity in nuclear receptor transcriptional activation. *Genes Dev* 12:3357–3368
- Heery DM, Hoare S, Hussain S, Parker MG, Sheppard H 2001 Core LXXLL motif sequences in CREB-binding protein, SRC1, and RIP140 define affinity and selectivity for steroid and retinoid receptors. *J Biol Chem* 276: 6695–6702
- Ko L, Cardona GR, Iwasaki T, Bramlett KS, Burris TP, Chin WW 2002 Ser-884 adjacent to the LXXLL motif of coactivator TRBP defines selectivity for ERs and TRs. *Mol Endocrinol* 16:128–140
- Coulthard VH, Matsuda S, Heery DM 2003 An extended LXXLL motif sequence determines the nuclear receptor binding specificity of TRAP220. *J Biol Chem* 278: 10942–10951
- Chang C, Norris JD, Gron H, Paige LA, Hamilton PT, Kenan DJ, Fowlkes D, McDonnell DP 1999 Dissection of the LXXLL nuclear receptor-coactivator interaction motif using combinatorial peptide libraries: discovery of peptide antagonists of estrogen receptors  $\alpha$  and  $\beta$ . *Mol Cell Biol* 19:8226–8239
- Chang CY, McDonnell DP 2002 Evaluation of ligand-dependent changes in AR structure using peptide probes. *Mol Endocrinol* 16:647–660
- Dubbink HJ, Hersmus R, Verma CS, van der Korput HAGM, Berrevoets CA, van Tol J, Ziel-van der Made ACJ, Brinkmann AO, Pike ACW, Trapman J 2004 Distinct recognition modes of FXXLF and LXXLL motifs by the androgen receptor. *Mol Endocrinol* 18:2132–2150
- Hur E, Pfaff SJ, Payne ES, Gron H, Buehrer BM, Fletterick RJ 2004 Recognition and accommodation at the androgen receptor coactivator binding interface. *PLoS Biol* 2:E274
- He B, Kempainen JA, Wilson EM 2000 FXXLF and WXXLF sequences mediate the NH<sub>2</sub>-terminal interaction with the ligand binding domain of the androgen receptor. *J Biol Chem* 275:22986–22994
- He B, Minges JT, Lee LW, Wilson EM 2002 The FXXLF motif mediates androgen receptor-specific interactions with coregulators. *J Biol Chem* 277:10226–10235
- Wang L, Hsu CL, Ni J, Wang PH, Yeh S, Keng P, Chang C 2004 Human checkpoint protein hRad9 functions as a negative coregulator to repress androgen receptor transactivation in prostate cancer cells. *Mol Cell Biol* 24: 2202–2213

29. He B, Gampe Jr RT, Kole AJ, Hnat AT, Stanley TB, An G, Stewart EL, Kalman RI, Minges JT, Wilson EM 2004 Structural basis for androgen receptor interdomain and coactivator interactions suggests a transition in nuclear receptor activation function dominance. *Mol Cell* 16: 425–438
30. Estebanez-Perpina E, Moore JM, Mar E, Delgado-Rodriguez E, Nguyen P, Baxter JD, Buehrer BM, Webb P, Fletterick RJ, Guy RK 2005 The molecular mechanisms of coactivator utilization in ligand-dependent transactivation by the androgen receptor. *J Biol Chem* 280: 8060–8068
31. Feldman BJ, Feldman D 2001 The development of androgen-independent prostate cancer. *Nat Rev Cancer* 1:34–45
32. Scher HI, Buchanan G, Gerald W, Butler LM, Tilley WD 2004 Targeting the androgen receptor: improving outcomes for castration-resistant prostate cancer. *Endocr Relat Cancer* 11:459–476
33. Hsu CL, Yeh S, Chen YL, Ting HJ, Hu YC, Lin H, Wang X, Chang C 2003 The use of phage display technique for the isolation of androgen receptor interacting peptides with F/WXXLF/W and FXXLY new signature motifs. *J Biol Chem* 278:23691–23698
34. Chang CY, Abdo J, Hartney T, McDonnell DP 2005 Development of peptide antagonists for the androgen receptor using combinatorial peptide phage display. *Mol Endocrinol* 19:2478–2490
35. Northrop JP, Nguyen D, Piplani S, Oliván SE, Kwan ST, Go NF, Hart CP, Schatz PJ 2000 Selection of estrogen receptor  $\beta$ - and thyroid hormone receptor  $\beta$ -specific coactivator-mimetic peptides using recombinant peptide libraries. *Mol Endocrinol* 14:605–622
36. Hu YC, Yeh S, Yeh SD, Sampson ER, Huang J, Li P, Hsu CL, Ting HJ, Lin HK, Wang L, Kim E, Ni J, Chang C 2004 Functional domain and motif analyses of androgen receptor coregulator ARA70 and its differential expression in prostate cancer. *J Biol Chem* 279:33438–33446
37. Darnell Jr JE 2002 Transcription factors as targets for cancer therapy. *Nat Rev Cancer* 2:740–749
38. Vassilev LT, Vu BT, Graves B, Carvajal D, Podlaski F, Filipovic Z, Kong N, Kammloft U, Lukacs C, Klein C, Fotouhi N, Liu EA 2004 In vivo activation of the p53 pathway by small-molecule antagonists of MDM2. *Science* 303:844–848
39. Oltersdorf T, Elmore SW, Shoemaker AR, Armstrong RC, Augeri DJ, Belli BA, Bruncko M, Deckwerth TL, Dinges J, Hajduk PJ, Joseph MK, Kitada S, Korsmeyer SJ, Kunzer AR, Letai A, Li C, Mitten MJ, Nettesheim DG, Ng S, Nimmer PM, O'Connor JM, Oleksijew A, Petros AM, Reed JC, Shen W, *et al.* 2005 An inhibitor of Bcl-2 family proteins induces regression of solid tumours. *Nature* 435:677–681
40. Doesburg P, Kuil CW, Berrevoets CA, Steketeer K, Faber PW, Mulder E, Brinkmann AO, Trapman J 1997 Functional in vivo interaction between the amino-terminal, transactivation domain and the ligand binding domain of the androgen receptor. *Biochemistry* 36:1052–1064
41. Jenster G, Spencer TE, Burcin MM, Tsai SY, Tsai MJ, O'Malley BW 1997 Steroid receptor induction of gene transcription: a two-step model. *Proc Natl Acad Sci USA* 94:7879–7884
42. Gietz D, St Jean A, Woods RA, Schiestl RH 1992 Improved method for high efficiency transformation of intact yeast cells. *Nucleic Acids Res* 20:1425
43. Steketeer K, Timmerman L, Ziel-van der Made AC, Doesburg P, Brinkmann AO, Trapman J 2002 Broadened ligand responsiveness of androgen receptor mutants obtained by random amino acid substitution of H874 and mutation hot spot T877 in prostate cancer. *Int J Cancer* 100:309–317



**Molecular Endocrinology** is published monthly by The Endocrine Society (<http://www.endo-society.org>), the foremost professional society serving the endocrine community.